Chin. J. Astron. Astrophys. Vol. 8 (2008), **Supplement**, 165–168
(*http://www.chjaa.org*)

Chinese Journal of
Astronomy and
Astrophysics

X-Ray Spectroscopy of SN1006 with *Suzaku*

Katsuji Koyama[1], Hiroya Yamaguchi[1] and Aya Bamba[2]

[1] Department of Physics, Kyoto University, Sakyo-ku, Kyoto, 606-8502, Japan
[2] Institute of Space and Astronautical Science, JAXA, 3-1-1 Yoshinodai, Sagamihara, Kanagawa 229-8510, Japan

Abstract We report the *Suzaku* results on the structures of the thermal plasmas and non-thermal emissions from SN 1006, a type Ia supernova remnant. Clear evidence for a type Ia SNR is found in the metal abundances of the ejecta. Stringent constraint on the maximum electron energy and the synchrotron loss time are given from the non-thermal spectrum.

1 INTRODUCTION

From the historical records, SN 1006 is regarded to be one of the Galactic type Ia supernova remnants (SNRs). Type Ia SNe produce a large amount of iron compared to core-collapsed SNe (Type II) (e.g. Nomoto et al. 1984; Iwamoto et al. 1999). As for SN1006, however no clear iron line has been so far found. This is possibly due to extreme non-equilibration of the shock-heated plasma (Vink et al. 2000, 2003). The extreme non-equilibration indicates that SN 1006 is the 'youngest' even though the real age is $\sim$3 times older than the other known historical SNRs (e.g. Cas A, Kepler and Tycho). Therefore detailed study of thermal spectrum of SN1006 is highly desired for the understanding of the evolution of early stage of young SNR.

On the other hand, a hint of the cosmic ray acceleration is reported from the shell of the SN 1006 (Koyama e al. 1995). A key observation is to determine a roll-off energy, which gives the maximum energy of accelerated electrons and the magnetic field.

In this paper, we report the first results of the wide-band *Suzaku* (Mitsuda et al. 2007) observations of SN 1006. We assume the distance of SN 1006 to be 2.17 kpc (Winkler et al. 2003), and quoted errors are the 90% confidence level, unless otherwise stated.

2 OBSERVATIONS AND DATA REDUCTION

Suzaku has one Hard X-ray Detector (HXD; Takahashi et al. 2007; Kokubun et al. 2007), and four X-ray Imaging Spectrometers (XIS; Koyama et al. 2007) placed on the focal planes of four X-Ray Telescopes (XRT; Serlemitsos et al. 2007). For the studies on the thermal and non-thermal spectra, we utilized the best *Suzaku* performances: the high energy resolution and large effective area in the 2–12 keV band (the XIS with Front Illuminated: FI CCD) and the low energy band below 2 keV (Back Illuminated: BI CCD), and the high energy sensitivity of the silicon PIN diode array in the HXD system. The details of the operation modes, data reductions, and background subtractions for the XIS and PIN of the SN 1006 observations are given by Yamaguchi et al. (2007) and Bamba et al. (2007).

3 THERMAL EMISSION

We found that the spectra from the southeast region of SN 1006 exhibits clear K-shell (Kα) lines from Ar, Ca, and Fe, for the first time. With a power-law plus Gaussian-line fit, we determined the line center energy of the Fe-Kα to be $\sim$6.43 keV. This energy constrains the Fe ionization state to be less than Ne-like. Since

⋆ E-mail: koyama@cr.scphys.kyoto-u.ac.jp

the Fe-Kα line is a key for the study of the SN 1006 plasma, detailed analyses hereafter are made using the Fe-brightest part in the southeast region.

The spectra, in particular the line profiles are complicated. We therefore derived the plasma parameters separately from the three-energy band data: the low energy band for the light elements (O and Ne), the medium energy band for Mg, Si and S, and the high energy band for heavy elements (Ar, Ca and Fe).

As a result, three VNEI (Variable abundance Non Equilibrium Ionization) components are required; (1) high-kT_e ($1-2$ keV) with high-n_et ($\sim 10^{10}$ cm^{-3} s) and (2) with low-n_et ($\sim 10^{9}$ cm^{-3} s), and (3) low-kT_e (~ 0.6 keV) with medium-n_et ($\sim 6\times10^{9}$ cm^{-3} s). Since the component (3) does not require non-solar abundance, we fixed the abundance to be solar. For the other components, (1) and (2), we set the abundances as free parameters.

With these parameters as initial values, we fit the full energy range spectra with 3-NEI components model, but the model is rejected with the best-fit χ^2/d.o.f. of 1201/821. We found a systematic data excess at energies of $>$4 keV. This may be due to additional non-thermal component. Therefore, we added a power-law model for the hard X-rays. Then the fit was significantly improved with χ^2/d.o.f. = 1031/819. The best-fit parameters are shown in Table 1, while the best-fit model in the full energy band is shown in Figure 1.

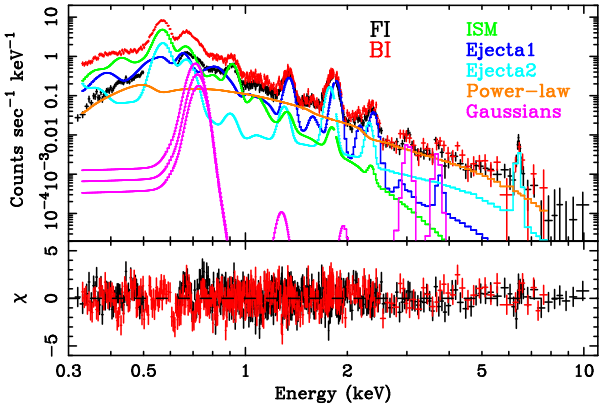

Fig. 1 The XIS spectra in the 0.33–10 keV band from the iron K-shell line dominant part in the southeast of the SNR. The best-fit model is also shown.

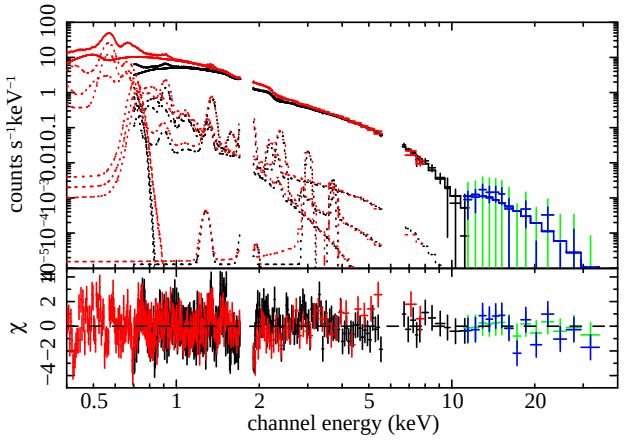

Fig. 2 Wide band spectra of XIS and PIN from the northeast and southwest non-thermal rims. The best-fit models are also shown.

4 NON-THERMAL EMISSION

We made combined XIS spectra from the NE and SW rim regions. In addition to strong emission lines below 2 keV, a hard component is clearly detected up to 12 keV. Therefore, we fitted the spectra using thermal plasma components plus a power-law continuum. As for the thermal component, we use the best-fit model obtained in Section 3 except for the normalization, but fine-tuned to get the best-fit. The non-thermal component cannot be represented by a simple power-law model. The residuals have a wavy structure in the high energy band. We accordingly introduced the *srcut* model (Reynolds 1998), which gives a largely improved reduced χ^2.

We next added the PIN spectrum. Figure 2 shows the wide-band spectra in the 0.4–40.0 keV band, where the ratio of the normalization constant between XIS and PIN has been fixed at 1.15 (Kokubun et al. 2007). The solid and dotted lines represent the best-fit model (thermal + *srcut* model). The non-thermal component is smoothly connected from the XIS band to the PIN band.

5 DISCUSSION

5.1 Origin of the Plasmas

We found that the thermal spectra are composed of three thin-thermal plasmas in non-equilibrium ionization (VNEI 1, VNEI 2 and NEI, in Table 1). Since the model NEI has solar abundances, the origin is likely a shock-heated interstellar medium (ISM). The low energy X-rays, in particular Kα lines from OVII and OVIII, are mainly due to this component.

Table 1 Best-fit Parameters for Thermal Emission

Component	Parameter	Value
Absorption	$N_{\rm H}$ (cm^{-2})	6.8×10^{20} (fixed)
VNEI 1 (Ejecta 1)	kT_e (keV)	1.2 (1.1–1.4)
	n_et (cm^{-3} s)	1.4 (1.2–1.6) ×10^{10}
VNEI 2 (Ejecta 2)	kT_e (keV)	1.9 (1.5–2.6)
	n_et (cm^{-3} s	7.7 (6.7–9.2) ×10^{8}
NEI (ISM)	kT_e (keV)	0.51(0.31–0.55)
	n_et (cm^{-3} s)	5.8 (5.7–6.1) ×10^{9}
χ^2/d.o.f.		1031/819=1.26

The other plasmas, VNEI 1 and VNEI 2 are highly over-abundant in heavy elements, hence would be ejecta origin. Since VNEI 1 has a larger ionization parameter of $\sim 10^{10}$ cm^{-3} s than VNEI 2, we interpret this plasma is heated by reverse shock in the early stage of the remnant evolution (here Ejecta 1). VNEI 2 has an extremely low ionization parameter of $\sim 10^{9}$ cm^{-3} s, and hence would be heated much more recently (here Ejecta 2). From this plasma, we have detected clear iron Kα line for the first time.

5.2 Relative Abundance in the Ejecta

In Figure 3, we compare the relative abundances with those of the Ia model, W7 (Nomoto et al. 1984). In the case of Ejecta 1, although the abundances of C, Ne, Mg, Si and S relative to O are almost consistent with the W7 model, those of Ca and Fe are much lower than the predicted values (Fig. 3a). Ejecta 2, on the other hand, has large amount of the heavy elements, which is consistent with the W7 model (Fig. 3b). These results can be interpreted that the heavier elements are preferentially located in the inner layers of the remnant unlike the lighter elements, and hence heavier elements are more recently heated by the reverse shock.

5.3 Low ISM density and Ionization Parameter

The best-fit ionization parameter (n_et) in the ISM plasma is 5.8×10^9 cm^{-3} s. From the emission measure (*EM*), we estimated the electron density (n_e) to be $0.17\ (0.16 - 0.24)$ cm^{-3}. Since the age of SN 1006 is $\sim$1000 yr, ionization parameter can be roughly estimated to be $n_et \sim 5.5 \times 10^9$ cm^{-3} s, which is consistent with the best-fit value. These low ISM density and ionization parameters put SN 1006 to be effectively the 'youngest' Galactic SNR in terms of the thermal plasma structure.

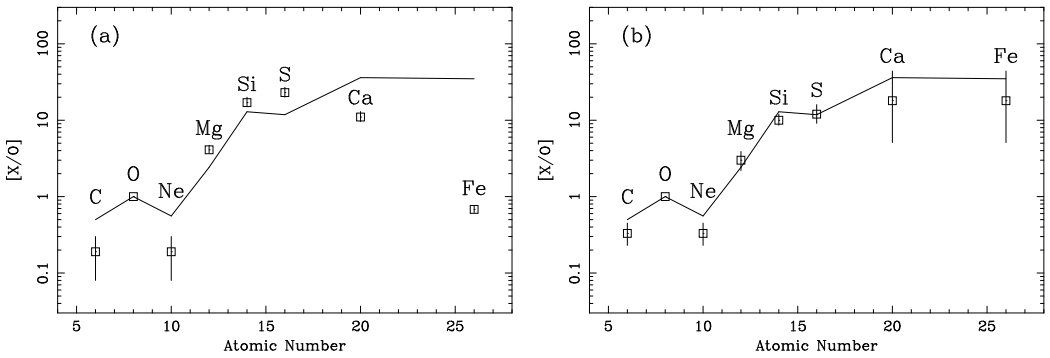

Fig. 3 Metal abundances of Ejecta 1 (a) and Ejecta 2 (b). The solid lines show the abundances relative to oxygen in the W7 model for a type Ia supernova by Nomoto et al. (1984).

5.4 Power-Law Emissions

An *srcut* model provides better fit than a power-law model. The roll-off energy is $5.69(5.67-5.71)\times10^{16}$ Hz (~ 0.23 keV), which is the most precise measurement to date. The roll-off energy $\nu_{\rm roll}$ is given by

$$\nu_{\rm roll} = 1.6 \times 10^{16} \left(\frac{B}{10\ \mu{\rm G}}\right) \left(\frac{E_e}{10\ {\rm TeV}}\right)^2 \ , \qquad (1)$$

where E_e and B are the maximum energy of accelerated electrons and the magnetic field, respectively. Then the maximum energy of electrons is estimated to be 9.4 TeV, under the assumption of the downstream magnetic field of 40 μG (Bamba et al. 2003).

The time scale of the synchrotron loss is estimated as

$$\tau_{\rm loss} = 2.0 \times 10^4 \left(\frac{B}{10\ \mu{\rm G}}\right)^{-2} \left(\frac{E_e}{10\ {\rm TeV}}\right) \ [{\rm yr}] \ . \qquad (2)$$

Then we find that $\tau_{\rm loss}$ is $\sim$1300 yr, roughly the same as the SNR age. This implies that the electron acceleration in SN 1006 is changing from age-limited to synchrotron-loss limited.

Acknowledgements We are grateful to all the members of the Suzaku hardware and software teams and the science working group. This work is supported by the Grant-in-Aid for the 21st Century COE "Center for Diversity and Universality in Physics" from Ministry of Education, Culture, Sports, Science and Technology (MEXT) of Japan.

References

Bamba A., Yamazaki R., Ueno M., Koyama K., 2003, ApJ, 589, 827
Bamba A. et al., 2007, PASJ, 59, submitted
Iwamoto K., Brachwitz F., Nomoto K., Kishimoto N., Umeda H., Hix W. R., Thielemann F.-K.. 1999, ApJS, 125, 439
Kokubun M., et al., 2007, PASJ, 59, 53
Koyama K., Petre R., Gotthelf E. V., Hwang U., Matsuura M., Ozaki M., Holt S. S., 1995, Nature, 378, 255
Koyama K., et al., 2007, PASJ, 59, 23
Mitsuda K., et al., 2007, PASJ, 59, 1
Nomoto K., Thielemann F.-K., Yokoi K., 1984, ApJ, 286, 644
Reynolds S. P., Keohane J. W., 1999, ApJ, 525, 368
Serlemitsos P. J., et al., 2007, PASJ, 59, 9
Takahashi T., et al., 2007, PASJ, 59, 35
Vink J., Kaastra J. S., Bleeker J. A. M., Preite-Martinez A., 2000, A&A, 354, 931
Vink J., Laming J. M., Gu M. F., Rasmussen A., Kaastra J. S., 2003, ApJ, 587, L31
Winkler P. F., Gupta G., Long K. S., 2003, ApJ, 585, 324
Yamaguchi H. et al., 2007, PASJ, 59, accepted, (astro-ph 07064146)